Applied Catalysis B: Environmental 185 (2016) 31–41

Contents lists available at ScienceDirect

Applied Catalysis B: Environmental

journal homepage: www.elsevier.com/locate/apcatb

Decomposition of sulfadiazine in a sonochemical Fe^0-catalyzed persulfate system: Parameters optimizing and interferences of wastewater matrix

Tao Zhou*, Xiaoli Zou, Juan Mao, Xiaohui Wu**

School of Environmental Science and Engineering, Huazhong University of Science and Technology, Wuhan 430074, PR China

ARTICLE INFO

Article history:
Received 14 September 2015
Received in revised form
18 November 2015
Accepted 2 December 2015
Available online 4 December 2015

Keywords:
Sonochemical Fenton-like
Fe^0-persulfate
Response surface methodology
Inorganic anions
Chelating agents

ABSTRACT

Effective decomposition of antibiotic sulfadiazine (SD) in a Fe^0-catalyzed sonochemical Fenton like system (Sono-FL) was demonstrated. By using the response surface methodology (RSM), an optimized experimental condition of pH 7.00, 0.94 mM Fe^0, 1.90 mM persulfate (PS) and 20 W ultrasound (US) power was concluded, which could reach the predicted SD degradation efficiency of 90%. Afterwards, effects of wastewater matrix (five inorganic anions and two chelating agents) on the SD degradation were investigated in the system, respectively. It was found that the SD degradation could be inhibited by SO_4^{2-}, NO_3^-, HCO_3^-/CO_3^{2-} and $H_2PO_4^-$ to different extents. Cl^- would lead to an enhancement with a low dosage (5 mM), but an inhibition with a high dosage (100 mM). Unexpectedly, chlorinated organic intermediates were also found as SD decomposed. Appropriate dosages of oxalic acid (OxA) or EDTA could benefit the SD degradation in the Sono-FL system, while excessive chelating agents would play as competitive pollutants. It was summarized that inorganic anions would mainly react with $SO_4^{\bullet-}$ and/or •OH to form sub-radicals of less oxidative potential. OxA and EDTA would not only participate in complexing dissolution of Fe^0 but also provide additional oxidants such as H_2O_2 and $[Fe^{IV}O]^{2+}$, through the electron transfer reactions caused by the iron-ligands species.

1. Introduction

Nowadays, advanced oxidation processes (AOPs) have been already regarded as good alternatives to biological treatment processes for the treatment of recalcitrant organic pollutants such as pesticides, textile and pharmaceuticals wastewaters [1,2]. Many common AOPs e.g., photolysis [2], Fenton process [3] and ozonation [4] are aqueous oxidation processes basing on the hydroxyl radical (•OH) with a high oxidation potential of 2.8 V [5]. Through directly attacking the molecule structures, •OH could decompose most bio-recalcitrant organics and thus improve their biodegradability effectively [2–4,6]. Nevertheless, it should be noticed that •OH-based AOPs usually suffer from their narrow work pH range, and the short life span of the radical (less than 1 μs) [5,7].

It has been reported that another oxidant i.e., sulfate radical ($SO_4^{\bullet-}$) could be an attractive substitution for •OH. Possessing a high oxidation potential (2.5–3.1 V vs. NHE), $SO_4^{\bullet-}$ is generally supposed to have a longer life span of 30-40 μs [7]. This enables $SO_4^{\bullet-}$ to be more stable than •OH in reacting with target pollutants. Besides, $SO_4^{\bullet-}$-based AOPs could oxidize organic compounds efficiently over a wide pH range of 2–8 [8]. Generally, $SO_4^{\bullet-}$ can be generated by radiolysis, photolysis, pyrolysis or chemical activation (various transition metallic ions) of persulfate (PS, $S_2O_8^{2-}$) or peroxymonosulfate [7,9–16]. Among these methods, adopting Fe^0 to activate PS was attractive, since the heterogeneous Fe^0/PS Fenton-like system could achieve a good performance, which is even superior to traditional Fenton reaction at neutral pHs with lower dosage of reagents [8,17–21]. In addition, the Fe^0/PS system could also couple with several physiochemical methods such as ultrasound [8,22], weak magnetic field [23] and bimetals [24], to overcome the heterogeneous mass transfer barrier and obtain much better efficiency in organics decomposition.

Operation of AOPs with efficient and cost-effective ways are generally critical to their practical applications. In order to achieve a propriety application condition, Response surface methodology (RSM) was used. RSM is popular and well-accepted statistical and mathematical technique for the development, improvement and optimization of certain processes [6]. Compared to conventional optimization methods, RSM is economic and time-saving since it

* Corresponding author. Fax: +86 27 87792101.
** Corresponding author.
E-mail addresses: zhoutao@hust.edu.cn (T. Zhou), xhwoo@hust.edu.cn (X. Wu).

http://dx.doi.org/10.1016/j.apcatb.2015.12.004
0926-3373/

can provide more information from much less number of experiments [25]. With respect to complex AOPs e.g., photocatalysis, sonication, electrochemical, empirical models developed by RSM have been widely and well addressed to describe interactive and synergistic effects of experimental variables as well as operation conditions optimization [26,27].

Besides, natural waters and industrial wastewaters commonly contain a lot of impurity substance including inorganic anions and chelating agents [28]. These impurities are regarded as great challenges for the practical application of many AOPs [29–31]. Numerous researches indicated that inorganic anions, e.g., NO_3^-, SO_4^{2-}, Cl^- and HCO_3^-, exhibited negative effects on the removal of target organic pollutants [10,29,30,32,33]. Performances of chelating agents should be rather complex during the treatment of aqueous organic compounds by AOPs, especially AOPs based on Fenton reaction [31,34,35]. In addition to their excellent complexion ability with iron ions, most of the formed iron-ligands could exhibit specific electron transferring and/or photochemical properties [36]. Several chelating agents such as oxalic acid and EDTA could present significant effects (enhancement or inhibition) on the Fenton-like oxidative degradation of different organic pollutants [31,37,38].

Previously, we have established a novel ultrasound-enhanced Fe^0/PS Fenton-like (Sono-FL) system and successfully achieved a significant synergistic degradation of antibiotic sulfadiazine. Unlike the classic AOPs, the Sono-FL system would be expected to work effectively in the presence of complex wastewater matrix, since $SO_4^{\bullet-}$-based AOPs could endure alkaline circumstances and relatively concentrated inorganic anions as compared to $^{\bullet}OH$-based AOPs [8,39]. The presence of inorganic anions could be also favorable to sonochemical systems to some extent [40]. Moreover, in such sonochemical Fenton-like systems, the interference of specific chelating agents should be not negligible [35,36,41].

Therefore, the target of this study is to offer a profound and systematic understanding in the interference of wastewater matrix put in the Sono-FL system. We were to: (a) optimize the operation parameters in the Sono-FL system by using RSM, (b) investigate the effects of 5 inorganic anions (Cl^-, SO_4^{2-}, NO_3^-, HCO_3^-/CO_3^{2-} and $H_2PO_4^-$) and two typical chelating agents (oxalate and EDTA) on the SD degradation, respectively, (c) and finally explore the interference roles of the complex wastewater matrix in the Sono-FL system.

2. Materials and methods

2.1. Materials

Purified sulfadiazine ($C_{10}H_{10}N_4O_2S$, ≥98%) was purchased from Aladdin China company. Analytical grade Na_2SO_4 (≥99.8%), NaCl (99.5%), $NaNO_3$ (99.0%), NaH_2PO_4 (99.5%), Na_2CO_3 (99.9%), $NaHCO_3$ (99.9%), $Na_2(C_2O_4)$ (99.8%), Na_2EDTA (99.0%), micrometric iron powder (Fe^0 ≥ 99%, 100 mesh, with a mean particle size of ~150 mm), methanol (MA, ≥99.5%), CH_3COONa (≥99%), and *tert*-butyl alcohol (TBA) were obtained from Sinopharm Chemical Reagent Co., Ltd (Shanghai, China). Potassium persulfate ($K_2S_2O_8$, PS) was acquired from Unite initiator Co., Ltd (Shanghai). Superoxide dismutase (SOD, 98% protein, 3000 U/mg protein) and catalase (CAT, 2000–5000 U/mg protein) were got from Biosharp company. All solutions in the study were prepared by deionized water.

2.2. Procedures

The sonochemical experimental set-up was described elsewhere [8]. In a typical experimental run, 400 mL reaction solution with a predetermined amount of SD and PS was put in a jacket-glass reactor. The reaction was started as the simultaneous addition of Fe^0 powder and switch on of the sonicator. The initial pH of the SD solution was adjusted by 0.1 M Sodium NaOH, HCl or $HClO_4$. During the reaction, the solution was stirred continuously and the reaction temperature was kept 20 ± 1 °C by a thermostat bath (DC-1015, Xinyi instrument, Ningbo). In the cases of wastewater matrix interfering, specific inorganic anions or organic chelates were added into the solution prior to the reaction. A 9 W fluorescent lamp or an air gas bubbling head was also used additionally in several specific cases. The scavenging experiments were initialized with the pre-addition of MA (100 mM), TBA (100 mM), SOD (1500 U/L) and CAT (150 mg/L) into the reactor, respectively. At the set intervals, samples were took out and filtered through 0.45 um membranes before analyzed.

2.3. Analysis

Sulfadiazine was quantified by a high performance liquid chromatography (HPLC, LC-15C, Shimadzu) equipped with a C18 column (4.6 × 25 cm) and a UV detector. A mixture of 0.02 mol L^{-1} sodium acetate (pH 4.75) and acetonitrile (V/V = 85%:15%) was adopted as the mobile phase with a flow rate of 0.8 mL min^{-1}. The detection wavelength and temperature were set at 275 nm and 30 °C, respectively. The SD degradation intermediates were examined by a HPLC-ESI-MS (Agilent 1100, USA). The mobile phase was a mixture of acetonitrile and water (V/V = 85%:15%) with a flow rate of 0.8 mL/min. The ESI-MS analysis was carried out with the ion-transfer capillary temperature of 300 °C and the spray voltage was 45 kV.

2.4. Experimental design strategy of response surface methodology (RSM)

According to the literatures [42,43], central composite design (CCD) was an excellent tool to establish RSM models, especially in the case of three level factorial designs. In a general case of CCD, the required number of experiment run can be expressed by an equation $N = k^2 + 2k + c_p$, where k and c_p represent the factor number and the replicate number of the central point, respectively. The value of key parameter α is depended on the number of variables, according to the equation of $\alpha = 2(k - c_p)/4$.

The software Design-Expert 8.0.6 (Stat-Ease Inc., USA) was used to design the experiments of SD degradation in the Sono-FL system. According to the previous literature [8], pH, Fe^0 dosage, PS dosage and US power were the important parameters affecting the SD degradation in the Sono-FL system. Therefore, the four CCD factors could be identified with 5 levels ($-\alpha, -1, 0, +1, +\alpha$). Then a series of experimental runs have been designed with the SD degradation efficiency as the response, as listed in Table 1.

3. Result and discussion

3.1. Parameters optimization using response surface methodology (RSM)

Table 1 shows the obtained actual responses (i.e., SD degradation efficiency) with respect to the 30 designed experiments. After the step-wise model fitting by the software, a cubic model for the SD degradation in the Sono-FL system could be concluded as expressed by Eq. (1), as a simultaneous function of pH (A), Fe^0 dosage (B), PS dosage (C) and US power (D).

$$\begin{aligned} \text{SDdegradationefficiency}(\%) = {} & 83.56 - 10.01A + 9.21B \\ & + 11.34C + 2.93D + 1.53AB - 1.48A^2 - 3.89B^2 - 1.30C^2 \\ & + 1.92D^2 - 8.72A^2B + 8.28AB^2 \end{aligned} \quad (1)$$

Table 1
The CCD design and response of SD degradation in the Sono-FL system.

Factors	Levels and ranges				
	$-\alpha$	Low (−1)	Middle (0)	High (+1)	$+\alpha$
A:pH	3.00	5.00	7.00	9.00	11.00
B:Fe^0 dosage (mM)	0.1	0.7	1.3	1.9	2.5
C:PS dosage (mM)	0.1	0.7	1.3	1.9	2.5
D:US Power (W)	20	50	80	110	140

Run	A (pH)	B (Fe^0 dosage)	C (PS dosage)	D (US power)	SD degradation%
1	5.00 (−1)	0.7 (−1)	0.7 (−1)	110 (+1)	75.62
2	5.00 (−1)	1.9 (+1)	0.7 (−1)	110 (+1)	70.47
3	9.00 (+1)	0.7 (-1)	0.7 (−1)	50 (−1)	60.93
4	7.00 (0)	1.3 (0)	1.3 (0)	80 (0)	83.24
5	7.00 (0)	2.5 (+α)	1.3 (0)	80 (0)	84.68
6	7.00 (0)	1.3 (0)	1.3 (0)	20 (−α)	81.66
7	7.00 (0)	1.3 (0)	1.3 (0)	80 (0)	83.18
8	5.00 (−1)	0.7 (−1)	1.9	50 (−1)	92.73
9	7.00 (0)	1.3 (0)	0.1 (-α)	80 (0)	56.37
10	7.00 (0)	1.3 (0)	1.3 (0)	80 (0)	84.35
11	9.00 (+1)	1.9(+1)	0.7 (−1)	50 (−1)	66.10
12	9.00 (+1)	1.9 (+1)	1.9 (+1)	50 (−1)	88.79
13	3.00 (−α)	1.3 (0)	1.3 (0)	80 (0)	95.94
14	9.00 (+1)	0.7(−1)	1.9 (+1)	50 (-1)	87.16
15	9.00 (+1)	0.7 (-1)	0.7 (-1)	110 (+1)	65.44
16	9.00 (+1)	1.9 (+1)	1.9 (+1)	110 (+1)	92.79
17	7.00 (0)	1.3 (0)	1.3 (0)	80 (0)	81.44
18	7.00 (0)	1.3 (0)	2.5 (+α)	80 (0)	96.90
19	7.00 (0)	0.1 (−α)	1.3 (0)	80 (0)	47.86
20	5.00 (−1)	1.9 (+1)	1.9 (+1)	110 (+1)	95.30
21	7.00 (0)	1.3 (0)	1.3 (0)	140 (+α)	97.39
22	11.00 (+α)	1.3 (0)	1.3 (0)	80 (0)	55.90
23	5.00 (−1)	1.9 (+1)	0.7 (−1)	50 (−1)	64.58
24	9.00 (+1)	0.7 (−1)	1.9 (+1)	110 (+1)	90.15
25	7.00 (0)	1.3 (0)	1.3 (0)	80 (0)	83.88
26	7.00 (0)	1.3 (0)	1.3 (0)	80 (0)	85.24
27	5.00 (−1)	0.7 (−1)	1.9 (+1)	110 (+1)	94.89
28	5.00 (−1)	1.9 (+1)	1.9 (+1)	50 (−1)	91.08
29	5.00 (−1)	0.7 (−1)	0.7 (−1)	50 (−1)	66.50
30	9.00 (+1)	1.9 (+1)	0.7 (−1)	110(+1)	72.10

Analysis of variance (ANOVA) of the obtained model can help us to identify the important factors, determine which one is the most significant and whether the experiment results are meaningful. As presented in Table 2, the corresponding ANOVA result indicated that the RSM model could be successfully applied for the SD degradation in the Sono-FL system. The model value of F and "Prob > F" were 73.97 and 0.0001, respectively. This indicated that the model and terms (<0.05) were significant and there was only a 0.01% chance that a "model F-value" could occur due to noise. It should be noted that the "lack of fit p-value" was 0.0526, suggesting that the lack of fit was not significant and the model had a good predictability. Besides, the value of R^2 and "Adeq precision" reached 0.98 and 31.42, respectively. It indicated that the model had a good degree of fitting and the signal to noise ratio was adequate (>4).

As the model established and optimized, it was found that interactive relationships between Fe^0 and PS (Eqs. (2)–(5)), pH and Fe^0 were significant in the Sono-FL system. The related 3D response surfaces could be plotted. From Fig. 1a, it can be seen that pH played an important role on the SD degradation in the system and acidic circumstance would be favorable. Moreover, optimal Fe^0 dosage could be observed under constant pH, especially in the cases of acidic conditions. It was in accordance with our previous finding that excessive generated Fe^{2+} would consume $SO_4^{\bullet-}$ competitively [8]. Fig. 1b illustrates the interactive relationship between Fe^0 and PS. An approximate optimal dosage ratio of [Fe^0]:[PS] was observed. Increasing the dosage of two chemicals in proportion would lead to gradual increase in the SD degradation efficiency. Nevertheless, as compared to the parameter PS dosage, Fe^0 dosage exhibited relative lower impacts at higher concentration levels, since the recycling of Fe^{2+} from Fe^{3+} on the surface of Fe^0, especially at low pH e.g., less than 4.0 (Eqs. (2)–(5)). This result suggested that we could adopt a relatively lower amount of Fe^0 with a certain PS dosage to achieve similar SD degradation efficiencies, while at high Fe^0 dosage, more iron corrosion products are produced which can result in more sludge in the solution and that is not very appropriate [12].

$$Fe^0 \rightarrow Fe^{2+} + 2e^- \quad (2)$$

$$Fe^0 + H_2O + 0.5O_2 \rightarrow Fe^{2+} + 2OH^- \quad (3)$$

$$Fe^0 + H_2O \rightarrow Fe^{2+} + 2OH^- + H_2 \quad (4)$$

$$S_2O_8^{2-} + Fe^{2+} \rightarrow SO_4^{2-} + SO_4^{\bullet-} + Fe^{3+} \quad (5)$$

According to the obtained RSM model, optimization of the four experimental parameters could be also conducted. Table 3 shows the constraints of each parameters. In accordance with the prac-

Table 2
ANOVA (analysis of variance) for the optimized RSM model.

Source	Sum of squares	df	Mean square	F Value	p-Value prob > F	
Model	5526.37	13	425.11	73.97	<0.0001	Significant
A-pH	801.60	1	801.60	139.49	<0.0001	
B-Fe^0 dosage	677.86	1	677.86	117.95	<0.0001	
C-PS dosage	3087.43	1	3087.43	537.25	<0.0001	
D-US power	206.21	1	206.21	35.88	<0.0001	
AB	37.24	1	37.24	6.48	0.0216	
BC	0.19	1	0.19	0.03	0.8591	
CD	9.23	1	9.23	1.61	0.2233	
A^2	60.02	1	60.02	10.44	0.0052	
B^2	415.43	1	415.43	72.29	<0.0001	
C^2	46.39	1	46.39	8.07	0.0118	
D^2	101.32	1	101.32	17.63	0.0007	
A^2B	405.36	1	405.36	70.54	<0.0001	
AB^2	365.48	1	365.48	63.60	<0.0001	
Residual	91.95	16	5.75			
Lack of fit	83.66	11	7.61	4.59	0.0526	Not significant
Pure error	8.29	5	1.66			
Cor total	5618.32	29				

Std. Dev.	2.39724286	R^2	0.9836342
Mean	79.7553333	R_{Adj}^2	0.970337
C.V.%	3.00574614	R_{Pred}^2	0.6403009
Press	2020.90453	Adeq precision	31.422977

Abbreviations: R^2—R-squared; R_{Adj}^2—adjusted R-squared; R_{Pred}^2—predicted R-squared; C.V.%—coefficient of variation; Std. Dev.—studentized range distribution.

Table 3
Optimization of the individual factors to obtain the overall desirability response.

Name	Goal	Lower limit	Upper limit	Lower weight	Upper weight	Importance
A:pH	Is equal to 7.00	3	11	1	1	+++++
B:Fe^0 dosage	Is in range	0.7	1.9	1	1	+++++
C:PS dosage	Is in range	0.7	1.9	1	1	+++++
D:US power	Is equal to 20.00	20	90	1	1	++
SD degradation	Is target = 90	47.86	100	1	1	+++++

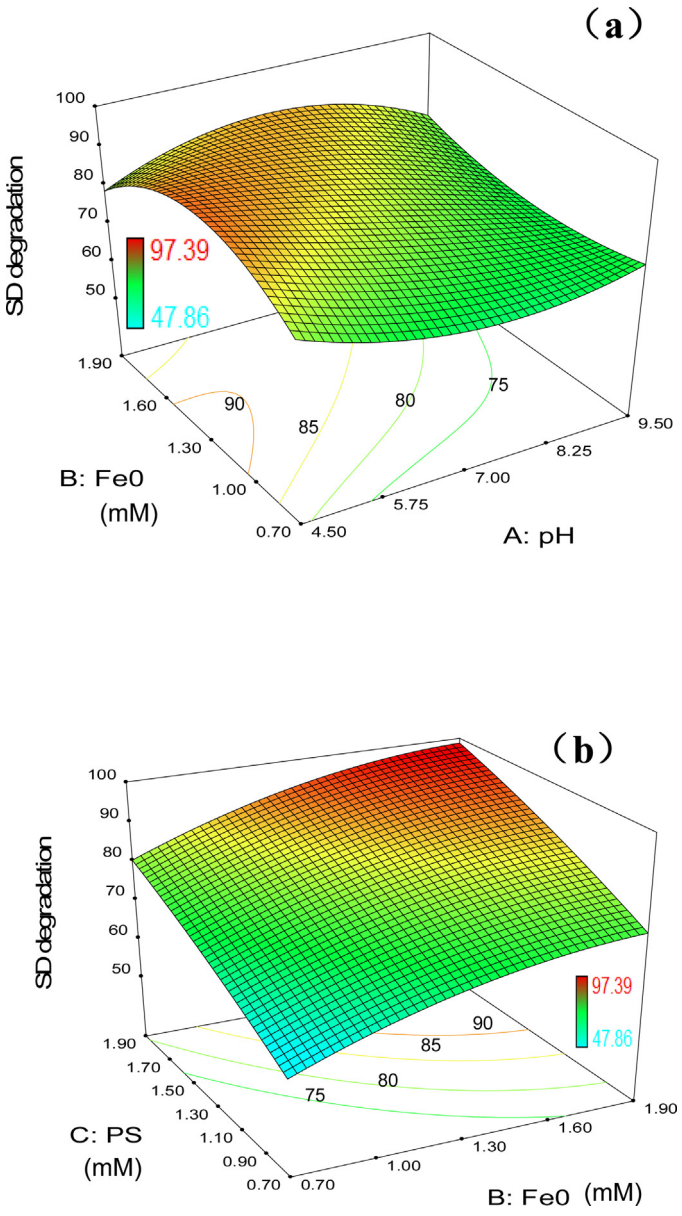

Fig. 1. Effects of the mutual interactions between (a) [PS] and [Fe^0], (b) initial pH and [Fe^0] with the 3D response surfaces for the SD degradation in the Sono-FL system.

tical wastewater treatments, the solution pH was set at 7.00 and US power was set at 20 W for achieving the lowest energy consumption. The left two parameters were set as "in range" due to their CCD levels. Targeting an expected SD degradation efficiency of 90%, an optimal condition of pH 7.00, 0.94 mM Fe^0, 1.90 mM PS and 20 W US power was predicted with a software calculated response of 89.9%. The verification experiment was then carried out under this optimized condition and an actual SD degradation efficiency of 93.2% was achieved. The result was in good agreement with the corresponding model prediction value, suggesting that the established model was robust and insensitive to external noise. Based on the obtained optimal experimental conditions, the interferences of water matrix were further investigated and discussed in the following sections.

3.2. Effects of common inorganic anions on the SD degradation in the Sono-FL system

3.2.1. Effects of SO_4^{2-}, NO_3^-, Cl^-, HCO_3^-/CO_3^{2-} and $H_2PO_4^-$

Effect of common inorganic anions in the Sono-FL system was evaluated under different conditions. Five inorganic anions (SO_4^{2-}, NO_3^-, HCO_3^-/CO_3^{2-}, $H_2PO_4^-$, Cl^-) were investigated, with two different initial concentrations of 5 mM and 100 mM, as well as two initial pH of 3.00 and 7.00, respectively. The corresponding results are shown in Fig. 2.

It was found that the SD degradation could be applied by the pseudo-first-order kinetic in the three cases of adding SO_4^{2-}, NO_3^- and Cl^-, respectively. As presented in Fig. 2a and b, the SD degradation rate would be slightly inhibited in the presence of 5 mM NO_3^-, under either initial pH 3.00 or 7.00. Concentrated NO_3^- (100 mM) would strongly inhibit the SD degradation. This is because more nitrate radical ($NO_3^{\bullet}$, 2–2.2 V) of less reactivity would be produced, as a result of the scavenging reaction between NO_3^- and oxidative radicals ($^{\bullet}OH/SO_4^{\bullet-}$) (Eqs. (6) and (7)) [44].

$$NO_3^- + SO_4^{\bullet-} \rightarrow NO_3^{\bullet} + SO_4^{2-}, k = 5.5 \times 10^5\ M^{-1}\ s^{-1} \quad (6)$$

$$NO_3^- + {}^{\bullet}OH \rightarrow NO_3^{\bullet} + OH^-, k < 5 \times 10^5\ M^{-1}\ s^{-1} \quad (7)$$

The presence of SO_4^{2-} could result in more serious inhibitions on the SD degradation. From Fig. 2a and b, it can be seen that the performance of existing SO_4^{2-} on the SD degradation was different in acidic and neutral circumstances. As compared to that in the blank system, the obtained k_{obs}(SD) were suppressed at about 5 and 31 times, in the cases of initial pH 3.00 with 5 mM and 100 mM SO_4^{2-}, respectively. However, the k_{obs}(SD) in the corresponding neutral cases were only suppressed about 3 and 8 times, respectively. The strong inhibitions caused by SO_4^{2-} could be mostly attributed to its influence on the oxidation reduction potential (ORP) of $SO_4^{\bullet-}/SO_4^{2-}$ [33]. Concentrated SO_4^{2-} could intensively decrease the ORP of $SO_4^{\bullet-}/SO_4^{2-}$, and lead to less efficient activation of PS. In addition, it was reported that $SO_4^{\bullet-}$ would be the dominant oxidant in acidic and neutral $SO_4^{\bullet-}$-based systems, while $^{\bullet}OH$ would become more responsible in the neutral systems [45]. Thus, the relative low inhibition observed in the neutral Sono-FL system could be explained by the reaction of SO_4^{2-} with $HO^{\bullet}$ which would generate $SO_4^{\bullet-}$ and increase the ORP of $SO_4^{\bullet-}/SO_4^{2-}$ (Eq. (8)).

$$HO^{\bullet} + SO_4^{2-}/HSO_4^- \rightarrow SO_4^{\bullet-} + OH^-/H_2O, k = 3.5 \times 10^5\ M^{-1}\ s^{-1} \quad (8)$$

Cl^- exhibited a complex effect on the SD degradation in the Sono-FL system (Fig. 2a and b). With 5 mM Cl^-, the SD degradation could be enhanced under initial pH of either 3.00 or 7.00. However, the presence of 100 mM Cl^- would negatively inhibit the SD degradation, especially in the neutral circumstance. In general, Cl^- can react with $SO_4^{\bullet-}$ or $^{\bullet}OH$ to generate sub-radicals such as $Cl^{\bullet}$, $Cl_2^{\bullet-}$ and $ClOH^{\bullet-}$ (Eqs. (11)–(13)) [32,46,47]. This process could

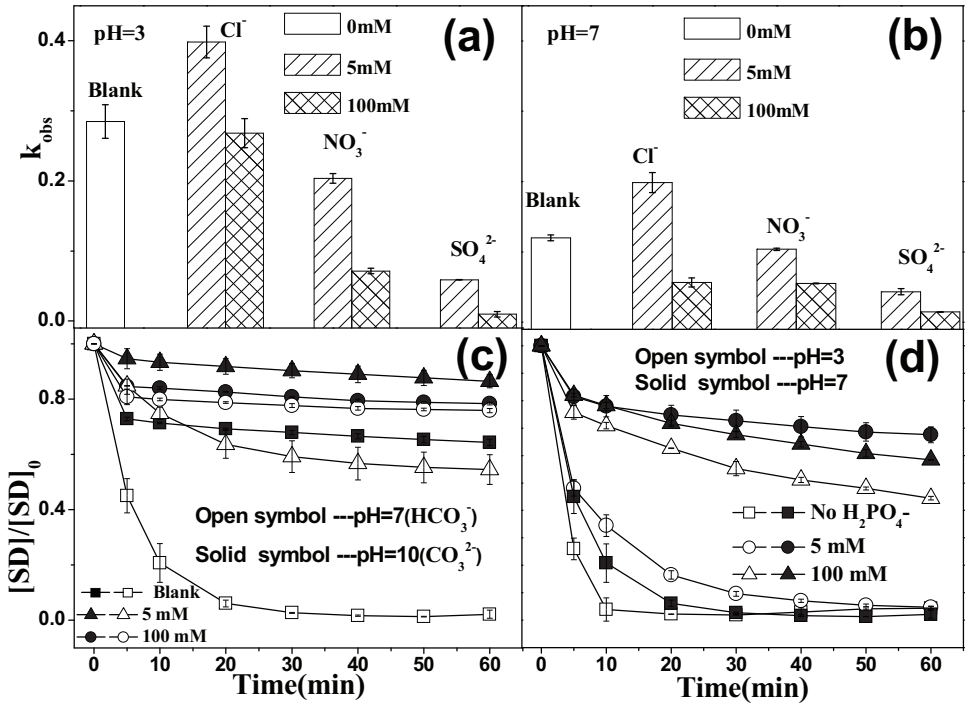

Fig. 2. Effects of five common inorganic ions (Cl^-, SO_4^{2-}, NO_3^-, HCO_3^-/CO_3^{2-} and $H_2PO_4^-$) on the SD degradation in the Sono-FL system (conditions: pH_0 3.00 or 7.00, $[anion]_0$ = 5, 100 mM, 20 mg L^{-1} SD, 1.90 mM PS, 0.94 mM Fe^0, 20 W US, 20 °C).

accelerate the decomposition of $S_2O_8^{2-}$ as well as avoid the scavenge reaction between $S_2O_8^{2-}$ and $SO_4^{\bullet-}$/•OH (Eqs. (9) and (10)). The enhanced SD degradation with low concentration of Cl^- could be therefore ascribed to the combining oxidation action of $SO_4^{\bullet-}$ and the reactive Cl species [46,48]. However, the produced $SO_4^{\bullet-}$ would be almost transformed into Cl• in the presence of concentrated Cl^-. After a series of electron transfer reactions between the reactive Cl species (Eqs. (11)–(15)), Cl_2 would be finally produced. The oxidative degradation of SD would be dominated by the reactive Cl species. Due to their lower ORP value (E ($Cl_2^{\bullet-}/Cl^-$) = 2.0 V, E ($Cl^\bullet/Cl^-$) = 2.4 V) than $SO_4^{\bullet-}$ [48,49], slight inhibition in the SD degradation would happen (Fig. 2a). In addition, 100 mM Cl^- would strongly retard the SD degradation in the neutral Sono-FL system (Fig. 2b). In this case, two main reactive radicals (•OH, $Cl_2^{\bullet-}$) could annihilate each other (Eqs. (14)–(16)). The scavenging effect of OH^- for the reactive Cl species (Eqs. (17) and (18)) would be an additional reason contributing to the inhibition of SD degradation.

$$S_2O_8^{2-} + {}^\bullet OH \rightarrow OH^- + S_2O_8^{\bullet-}, k = 6.1 \times 10^5\ M^{-1}\ s^{-1} \quad (9)$$

$$SO_4^{\bullet-} + S_2O_8^{2-} \rightarrow SO_4^{2-} + S_2O_8^{\bullet-}, k = 6.62 \times 10^5\ M^{-1}\ s^{-1} \quad (10)$$

$$SO_4^{\bullet-} + Cl^- \leftrightarrow SO_4^{2-} + Cl^\bullet, k = 2.47 \times 10^8\ M^{-1}\ s^{-1} \quad (11)$$

$$^\bullet OH + Cl^- \leftrightarrow HOCl^{\bullet-}, k_f = 6.1 \pm 0.8 \times 10^9\ M^{-1}\ s^{-1} \quad (12)$$

$$Cl^- + Cl^\bullet \leftrightarrow Cl_2^{\bullet-}, k_f = 8.0 \times 10^9\ M^{-1}\ s^{-1} \quad (13)$$

$$Cl_2^{\bullet-} + H_2O \rightarrow ClOH^{\bullet-} + Cl^- + H^+, k = 1.3 \times 10^3\ s^{-1} \quad (14)$$

$$Cl_2^{\bullet-} + Cl_2^{\bullet-} \rightarrow Cl_2 + 2Cl^-, k = 1.3 \times 10^9\ M^{-1}\ s^{-1} \quad (15)$$

$$^\bullet OH + Cl_2^{\bullet-} \rightarrow HOCl + Cl^-, k = 1.0 \times 10^9\ M^{-1}\ s^{-1} \quad (16)$$

$$OH^- + Cl_2^{\bullet-} \rightarrow HOCl^{\bullet-} + Cl^-, k = 4.0 \times 10^6\ M^{-1}\ s^{-1} \quad (17)$$

$$OH^- + Cl^\bullet \rightarrow ClOH^{\bullet-}, k = 1.8 \times 10^{10}\ M^{-1}\ s^{-1} \quad (18)$$

Since the addition of carbonate species would strongly influence the solution pH, the experiments of HCO_3^- and CO_3^{2-} were conducted at initial pH 7.00 and 10.00, respectively. As shown in Fig. 2c, the presence of 5 mM HCO_3^-/CO_3^{2-} exhibited a strong inhibition effect on the SD degradation in the Sono-FL system. It was because that HCO_3^-/CO_3^{2-} anions can rapidly scavenge $SO_4^{\bullet-}$ or •OH as expressed by Eqs. (19)–(22) [10,32]. The reactive carbonate species, i.e., $CO_3^{\bullet-}$ and $HCO_3^{\bullet-}$, are weak oxidant and hardly to oxidize the pollutant SD [32].

$$SO_4^{\bullet-} + CO_3^{2-} \rightarrow SO_4^{2-} + CO_3^{\bullet-}, k = 6.1 \times 10^6\ M^{-1}\ s^{-1} \quad (19)$$

$$^\bullet OH + CO_3^{2-} \rightarrow OH^- + CO_3^{\bullet-}, k = 3.9 \times 10^8\ M^{-1}\ s^{-1} \quad (20)$$

$$SO_4^{\bullet-} + HCO_3^- \rightarrow SO_4^{2-} + HCO_3^{\bullet-}, k = 9.1 \times 10^6\ M^{-1}\ s^{-1} \quad (21)$$

$$^\bullet OH + HCO_3^{2-} \rightarrow OH^- + HCO_3^{\bullet-}, k = 8.5 \times 10^8\ M^{-1}\ s^{-1} \quad (22)$$

Addition of 100 mM HCO_3^- or CO_3^{2-} could further retard the SD degradation. With the initial pH of 10.00, the dominant oxidant •OH [45] would be scavenged rapidly by concentrated CO_3^{2-} (main carbonate species at pH 10.00) at a high rate constant of $3.9 \times 10^8\ M^{-1}\ s^{-1}$ (Eq. (16)). With the initial pH of 7.00, a similar inhibition pattern of the SD degradation was observed, although HCO_3^- (main carbonate species at pH 7.00) can scavenge •OH more rapidly (Eq. (22)). In the case, both $SO_4^{\bullet-}$ and •OH would be dominant. According to Eqs. (21) and (22), $SO_4^{\bullet-}$ reacts with HCO_3^- at a speed two order of magnitude slower than the reaction between •OH and HCO_3^-. Therefore, $SO_4^{\bullet-}$ would be the responsible oxidant for the SD degradation in the neutral system with 100 mM carbonate present.

Fig. 2d shows the effect of phosphate ions on the SD degradation with initial pH of 3.00 or 7.00. At the initial pH of 3.00, the SD degradation would be slightly inhibited in the presence of 5 mM $H_2PO_4^-$, but strongly retard in the presence of 100 mM $H_2PO_4^-$. At the initial pH of 7.00, the SD degradation rate would be strongly suppressed with the addition of either 5 mM or 100 mM $H_2PO_4^-$. It was reported that the reaction rate between $H_2PO_4^-$ and $SO_4^{\bullet-}$ or •OH was immeasurably slow (Eqs. (23) and (24)) [50]. The generated phosphate radicals are also weak oxidant and unable to oxidize organic compounds effectively [51]. In addition, activation of PS would be blocked in the presence of concentrated phosphate

species, since phosphate could be adsorbed on the iron surface and thus inhibit the release of Fe^{2+} [11]. Phosphate could further complex with free Fe^{2+} to slow down the PS activation [52]. In neutral circumstances the PS-activation process would be more ineffective, due to the possible formation of iron-phosphate precipitates e.g., $Fe(H_2PO_4)_3$ [52].

$$H_2PO_4^- + SO_4^{\bullet-} \rightarrow SO_4^{2-} + H_2PO_4^{\bullet}, k < 7.0 \times 10^4\ M^{-1}\ s^{-1} \quad (23)$$

$$H_2PO_4^- + {}^{\bullet}OH \rightarrow OH^- + H_2PO_4^{\bullet}, k = (1-2) \times 10^4\ M^{-1}\ s^{-1} \quad (24)$$

3.2.2. Chlorinated degradation pathways of SD in the Sono-FL system with Cl^-

Through the HPLC-ESI–MS examination of the intermediates/products, we have found that the SD degradation pathways in the systems with SO_4^{2-}, NO_3^-, HCO_3^-/CO_3^{2-} and $H_2PO_4^-$ would be similar to that in the blank Sono-FL system as reported early [8]. However, the degradation of SD would be more complex in the case of Cl^- present. Ten organic intermediates were identified with the peak of *m/z* 97, *m/z* 173, *m/z* 187, *m/z* 219, *m/z* 214, *m/z* 257, *m/z* 261, *m/z* 270, *m/z* 252, *m/z* 273 and *m/z* 368, respectively. Hence, a scheme of SD degradation pathways was proposed as presented in Fig. 3. Three possible degradation pathways could be concluded as a result of the attack and co-actions of three types radicals, i.e., (a) •OH, (b) $SO_4^{\bullet-}$, and (c) reactive Cl species ($Cl^{\bullet}$ and $Cl_2^{\bullet-}$).

The first degradation pathway would go through the direct cleavage of S–N bond (β position) via •OH attacking, as evidenced by the detection of 2-aminopyrimide (*m/z* 97) and sulfanilamide acid (*m/z* 173) [9,53]. The two intermediates would react to form an intermediate with the peak of *m/z* 187, which could be further oxidized by $SO_4^{\bullet-}$ to the organic compound with peak at *m/z* of 219 [54].

The organic intermediate with peak of *m/z* 214 could be referred to 4-amino-N-carbaminmido-ylbenzensulfonamide (sulphaguanidine, $C_7H_{10}N_4O_2S$) [9,53]. The second pathway could be therefore suggested, as a result of $SO_4^{\bullet-}$ or •OH attacking of C—N bond (α position) in the pyrimidine ring of SD molecule [8]. The intermediate sulphaguanidine would be further oxidized by $SO_4^{\bullet-}$ and reactive Cl species, leading to the formation of two compound with peak of *m/z* of 257 and 261, respectively.

Besides, direct attack of SD by the reactive Cl species would also occur. The third degradation pathway would be initiated by the addition of Cl radical in the *para* position in the benzene ring of SD molecule, resulting in the formation of *para*-chlorosulfadiazine with peak of *m/z* 270. With the $SO_4^{\bullet-}$ oxidation, cleavage of γ position (C—N bonds in the pyrimidine ring) in the *para*-chlorosulfadiazine molecule would occur, followed by the Cl substitution in the pristine pyrimidine N position. The two compounds with the peak of *m/z* 252 and 273 were the corresponding chlorinated intermediates. Another chlorinated intermediate (*m/z* 368) was also detected, suggesting the combination reaction between 2-aminopyrimide (*m/z* 97) and the chlorinated compound of *m/z* 273.

With the continuous oxidation of the three types of radicals, ring opening of all intermediates would happen. Aliphatic acids with low molecule weight, and inorganic ions (e.g., NH_4^+, NO_3^- and SO_4^{2-}) would be the final mineralization products. Nevertheless, the appearance of chlorinated by-products should be unavoidable in the presence of reactive Cl species in this Sono-FL system [55].

3.3. Effects of typical chelating agents on the SD degradation in the Sono-FL system

Among the different types of chelating agents, amino carboxylic acid and hydroxyl carboxylic acid are most frequently-used [56]. Therefore, the corresponding classic chelating agents, i.e., oxalic acid and EDTA, were chosen to investigate their effects on the SD degradation in the Sono-FL system, respectively.

3.3.1. Oxalic acid (OxA)

Effect of OxA on the SD degradation in the Sono-FL system was investigated under various conditions. All the concerning data for SD degradation could be fitted with the pseudo-first-order kinetic. As shown in Fig. 4a, it was found that the SD degradation could be enhanced and then inhibited by increasing the [OxA]:[Fe^0] ratio gradually, with the initial pH of 3.00 and a fixed Fe^0 dosage of 0.94 mM in the dark circumstance. The k_{obs}(SD) increased from 0.28 min^{-1} to 0.41 min^{-1} with the increase of [OxA]:[Fe^0] ratio from 0 to 0.1, while it decreased rapidly to 0.014 min^{-1} as [OxA]:[Fe^0] was 2.0. Obviously, appropriate addition of OxA could be beneficial to the SD degradation. It was because that OxA could accelerate the iron corrosion and release of the dissolved iron species through its coordinating complexion on the Fe^0 surface [54,57]. The iron-oxalate complexes e.g., $Fe^{II}(C_2O_4)_2^{2-}$, $Fe^{III}(C_2O_4)_2^-$ and $Fe^{III}(C_2O_4)_2^{2-}$ are more stable than Fe^{2+} and Fe^{3+} in aqueous phase [57,58]. It was also reported that $Fe^{II}[(C_2O_4)_n]^{2-2n}$ presented more rapid electron transfer rate in catalyzing Fenton reaction [41,59]. Consequently, the complexing reaction between Fe^0 and OxA would effectively improve the activation of PS in the Sono-FL system. However, excessive addition of OxA would strongly retard the degradation of SD in the system. It was because that abundant oxalic molecules could occupied the adsorption sites on the surface of Fe^0, preventing the Fe^0 corrosion as well as the formation of aqueous iron-oxalate compounds [54]. Besides, concentrated OxA would become a competitive pollutant for the oxidative degradation of SD. Therein, the reactions (Eqs. (25)–(27)) between concentrated oxalate and $SO_4^{\bullet-}$/•OH would be also not ignored [60,61].

$$SO_4^{\bullet-} + C_2O_4^{2-} \rightarrow C_2O_4^{\bullet-} + SO_4^{2-}, k = 5.6 \times 10^6\ M^{-1}\ s^{-1} \quad (25)$$

$${}^{\bullet}OH + C_2O_4^{2-} \rightarrow CO_2^{\bullet-} + CO_2 + OH^-, k = 7.7 \times 10^6\ M^{-1}\ s^{-1} \quad (26)$$

Furthermore, to examine the contributions of additional in-situ generated radicals e.g., $C_2O_4^{\bullet-}$, the Sono-FL(OxA) system was investigated with light illumination or air aeration, respectively. Under the light illumination, a series of photochemical iron-oxalate reactions would be expected to occur, leading to additional production of •OH and regeneration of Fe^{II}-OxA species as depicted in Eqs. (27)–(32) [36,60].

$$Fe^{III}[(C_2O_4)_n]^{3-2n} + h\nu \rightarrow Fe^{II}[(C_2O_4)_n]^{2-2n} + C_2O_4^{\bullet-} \quad (27)$$

$$C_2O_4^{\bullet-} + O_2 \rightarrow 2CO_2 + O_2^{\bullet-} \quad (28)$$

$$O_2^{\bullet-} \leftrightarrow HO_2^{\bullet}(\text{pHdependent}) \quad (29)$$

$$O_2^{\bullet-}/HO_2^{\bullet} + H^+ \rightarrow H_2O_2 + O_2 \quad (30)$$

$$O_2^{\bullet-}/HO_2^{\bullet} + H^+ + Fe^{2+} \rightarrow H_2O_2 + O_2 + Fe^{3+} \quad (31)$$

$$Fe^{II}[(C_2O_4)_n]^{2-2n} + H_2O_2 \rightarrow Fe^{III}[(C_2O_4)_n]^{3-2n} + {}^{\bullet}OH + OH^- \quad (32)$$

$$Fe^{III}[(C_2O_4)_n]^{3-2n} + Fe^0 \rightarrow Fe^{II}[(C_2O_4)_n]^{2-2n} \quad (33)$$

However, as presented in Fig. 4b, illumination retarded slightly the SD degradation instead of improving it in the acidic Sono-FL system. While the air aeration seemed to bring insignificant effect on the k_{obs}(SD) with the initial pH of either 3.00 or 7.00. It was possibly due to the reduction of Fe^{III}-OxA complexes would much more easily occur on the abundant fresh Fe^0 surface, rather than by way of the photochemical reduction reaction (Eq. (33)).

To further understand the role of the reactive species in the Sono-FL(OxA) system, different scavengers were employed to investigate their effects on the SD degradation, respectively. Among the four scavengers, methanol (MA) could efficiently quench both •OH and $SO_4^{\bullet-}$, while *tert*-butyl alcohol (TBA) was just effective

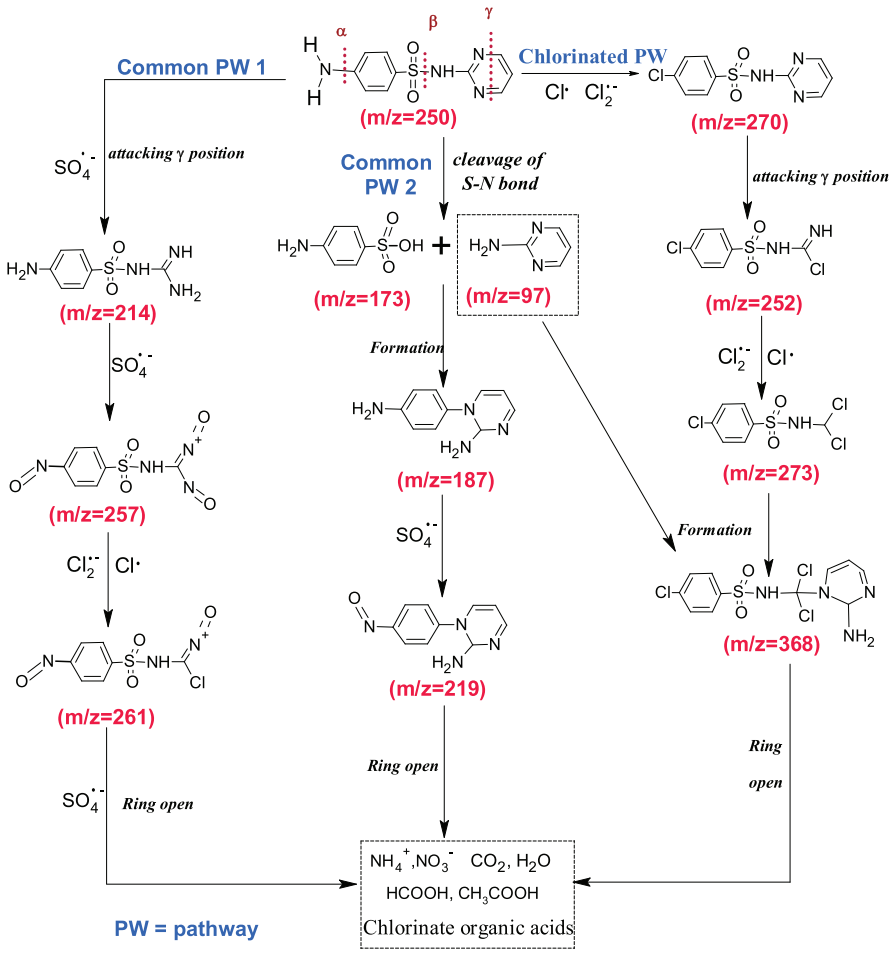

Fig. 3. The chlorinated pathway of SD degradation in the Sono-FL system with Cl^-.

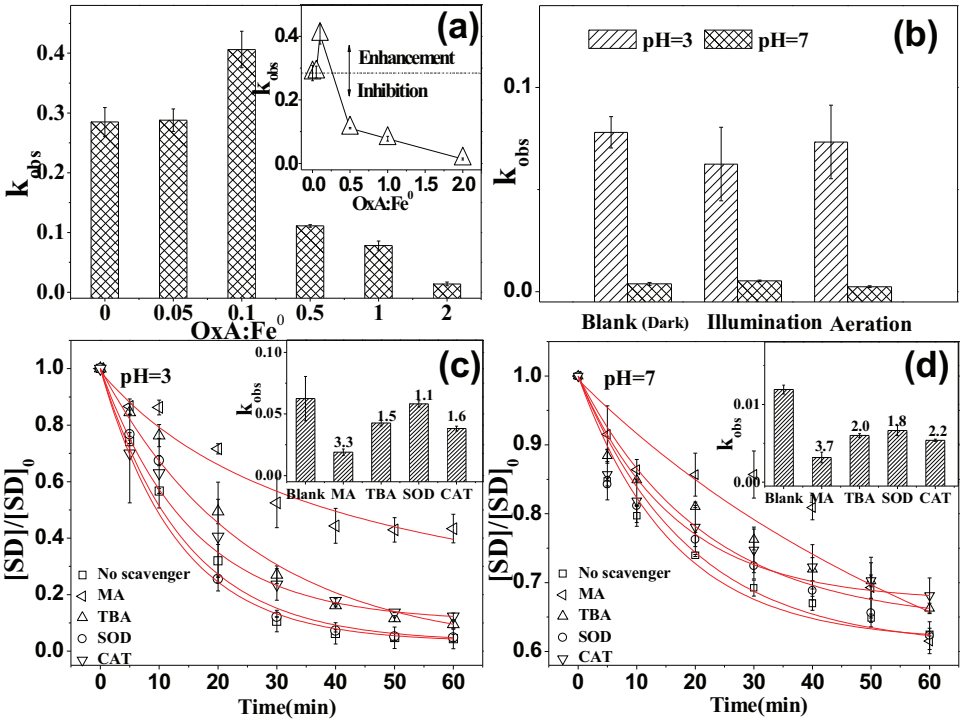

Fig. 4. Effect of (a) OxA dosage (pH_0 3), (b) illumination (9 W) and aeration, (c, d) 4 scavengers on the SD degradation in the Sono-FL system. Insets of (c, d): suppression ratios of SD degradation with the scavengers; (conditions: pH_0 3.00 or 7.00, 0.94 mM OxA, 20 mg L^{-1} SD, 1.90 mM PS, 0.94 mM Fe^0, 20 W US, 20 °C).

in quenching •OH ($k_{TBA/•OH}$ = 3.8–7.6 × 10^8 M^{-1} s^{-1}), but not for $SO_4^{•-}$ ($k_{TBA/SO4•-}$ = 8.0 × 10^5 M^{-1} s^{-1}) [62,63]. Superoxide dismutase (SOD) could be used as a scavenger for $O_2^{•-}$, and catalase (CAT) was chosen as a probe for H_2O_2 [64]. The results of scavenging experiments are exhibited in Fig. 4c and d, corresponding to the cases of initial pH 3.00 and 7.00, respectively. The suppression ratio of each scavenger expressed by $k_{obs}SD_{(Blank)}/k_{obs}SD_{(Scavenger)}$, is also listed in the insets Fig. 4c and d. Under the acidic condition, the sequence of the four scavengers in suppressing SD degradation was observed as MA > CAT > TBA > SOD. A much greater suppression ratio of 3.3 was achieved in the presence of MA, demonstrating that $SO_4^{•-}$ was the dominant oxidant for the SD degradation in the acidic Sono-FL system. Under the neutral condition, the sequence of suppression ratio was similar to that observed in the acidic case, but the inhibition in the k_{obs}(SD) became more intensive for all four scavengers. TBA and SOD were much more sensitive to the SD degradation in the neutral Sono-FL system, indicating the important role of the reactive oxygen species (i.e., •OH, $O_2^{•-}$ and H_2O_2). It was believable that •OH should be another main oxidant in addition of $SO_4^{•-}$ in the neutral Sono-FL system.

3.3.2. EDTA

As reported early [36,65], Fe^0/EDTA could effectively activate dissolved oxygen molecule to generate reactive species in-situ (Eqs. (34)–(39)). To clarify the contributions of different oxidative species for the SD degradation, the Sono-FL system with EDTA and air aeration was investigated and the results are presented in Fig. 5.

$$Fe^0 + O_2 + 2H^+ \rightarrow Fe^{2+} + H_2O_2 \quad (34)$$

$$Fe^{II}EDTA + O_2 \rightarrow Fe^{III}EDTA + O_2^{•-} \quad (35)$$

$$Fe^{II}EDTA + 2H^+ + O_2^{•-} \rightarrow Fe^{III}EDTA + H_2O_2 \quad (36)$$

$$Fe^{II}EDTA + H_2O_2 \rightarrow Fe^{III}EDTA + •OH + OH^- \quad (37)$$

$$Fe^{II}EDTA + S_2O_8^{2-} \rightarrow SO_4^{•-} + Fe^{III}EDTA \quad (38)$$

$$Fe^{II}EDTA + H_2O_2 \rightarrow [Fe^{IV}O]^{2+} + H_2O + EDTA \quad (39)$$

Fig. 5a and b exhibits the obtained k_{obs}(SD) values with different [EDTA]:[Fe^0] ratios and a fixed [Fe^0] of 0.94 mM, in the case with initial pH of 3.00 or 7.00, respectively. In the acidic cases, it can be seen from Fig. 5a that adding 0.019 mM EDTA (ratio = 0.05) could slightly improve the SD degradation, while further increasing the amount of EDTA would result in rapid and gradual decrease in the k_{obs}(SD). Obviously, due to its high chelating coefficients with Fe^{2+} and Fe^{3+} [37,66], a little amount of EDTA could accelerate the release of dissolved Fe(II) species from the Fe^0 surface. It would benefit to the activation of PS as well as the oxidative degradation of SD. But EDTA would be also a competitive pollutant for the $SO_4^{•-}$ oxidation [67]. Concentrated EDTA would not only compete with SD in consuming the generate $SO_4^{•-}$, but also form inert surface complexions on the Fe^0 surface [68]. Besides, reactive oxygen species (ROS) derived from Eqs. (34)–(38) could be subordinate oxidants for the SD degradation in the acidic circumstance, since the related reaction conditions were appropriate [65].

The effect of EDTA was more complex in the neutral Sono-FL(EDTA) system. As shown in Fig. 5b, the degradation of SD was suppressed in the most cases except the case with the lowest [EDTA]:[Fe^0] ratio of 0.05. Therein, a very low k_{obs}(SD) value of 0.001 min^{-1} was observed in the initial reaction phase of 30 min (phase1), followed by a rather rapid SD degradation (phase 2) of k_{obs}(SD) with 0.164 min^{-1} (the original degradation data are show in Appendices). Under neutral conditions activation of PS would be blocked in the initial reaction phase, since the EDTA species would be more easily adsorbed on the Fe^0 surface due to the electrostatic attraction [31]. With continuous coordination between EDTA and the formed iron oxides on the Fe^0 surface, aqueous Fe^{II}EDTA ligand would be generated [65], leading to efficient PS activation and rapid SD degradation.

Scavenging experiments were conducted likely to that in the case of OxA (Section 3.3.1). Fig. 5c and d illustrates the different k_{obs}(SD) values with the addition of the 4 different scavengers. The corresponding suppression ratios of the scavengers are also given in the insets in Fig. 5c and d. It can be seen that sequence of scavengers in suppressing the k_{obs}(SD) was MA > TBA > CAT > SOD and MA > TBA > SOD > CAT corresponding to the acidic circumstance and the neutral circumstance, respectively. It could be concluded that $SO_4^{•-}$ would be dominant in the acidic Sono-FL(EDTA) system, since the addition of MA inhibited the SD degradation significantly with a suppression ratio of 15.0 (Fig. 5d). •OH derived from Eqs. (35)–(37) would also participate in the SD degradation, as a result of the obvious inhibitions brought by the addition of TBA, SOD and CAT. The performances of the 4 scavengers were more interesting in the neutral circumstance. As seen in Fig. 5d, the suppression ratio was 6.6 in the case of adding MA, indicating that $SO_4^{•-}$ was not the only predominant oxidant. However, adding TBA, SOD and CAT would just cause slight inhibitions in the SD degradation. The related suppression ratio was 1.7, 1.2 and 1.1, respectively. This result suggested that an additional oxidant $[Fe^{IV}O]^{2+}$ instead of •OH would be the secondary oxidant for the SD degradation in the neutral Sono-FL(EDTA) system, according to early literatures [35,65].

3.4. Interference roles of the wastewater matrix in the Sono-FL system

According to the above results and the literatures [36,60,65], the mechanistic interference roles of the wastewater matrix for the SD degradation in the Sono-FL system could be incorporated and proposed as shown in Fig. 6.

The main reaction mechanism for the blank Sono-FL system has been reported elsewhere [8]. It contained a heterogeneous iron cycle in the Fe^0-water interphase and a homogeneous cycle of radical reactions in the bulk solution, both of which could be sonochemically accelerated. As presented in Fig. 6a, it was summarized that the five common inorganic anions (SO_4^{2-}, NO_3^-, HCO_3^-/CO_3^{2-}, $H_2PO_4^-$ and Cl^-) would mostly attend the cycle of radical reactions to affect the oxidative degradation of SD, in either acidic or neutral circumstance. The presence of SO_4^{2-}, NO_3^-, HCO_3^-/CO_3^{2-} and $H_2PO_4^-$ led to inhibitions on the SD degradation, whereas the effect of Cl^- was complex.

It was demonstrated that NO_3^- and HCO_3^-/CO_3^{2-} could act as scavengers of oxidative radicals (•OH/$SO_4^{•-}$), due to the production of less reactive oxidize radicals (i.e., NO_3•, $CO_3^{•-}$ and $HCO_3^{•-}$). SO_4^{2-} would suppress the SD degradation through decreasing the ORP of $SO_4^{•-}/SO_4^{2-}$ as well as scavenging •OH under the neutral condition. $H_2PO_4^-$ would be hardly to react with the radicals, but mostly interfered the release of Fe^{2+} and the activation of PS via forming iron-phosphate precipitates, especially in neutral circumstances. Nevertheless, Cl^- could react with $SO_4^{•-}$ or •OH to generate sub-chlorinated radicals (e.g., Cl• and $Cl_2^{•-}$). It would lead to an enhancement or inhibition on the SD degradation, with related to the presence of low or high concentration of Cl^-, respectively. Different from other four anions, additional chlorinated pathways for the SD degradation would occur with Cl^- present, resulting in the formation of harmful chlorinated products.

From Fig. 6b, it can be seen that the interference roles for the two types of chelating agent would be somewhat different. In the Sono-FL(OxA) system, the mechanism would be consist of three main parts, i.e., the complexion dissolution of Fe^0 (part I), the iron cycle and radical reactions (part II), and an additional photochemical iron cycle (part III). $SO_4^{•-}$ would be dominant in degrading SD in the acidic circumstance, while both $SO_4^{•-}$ and •OH would

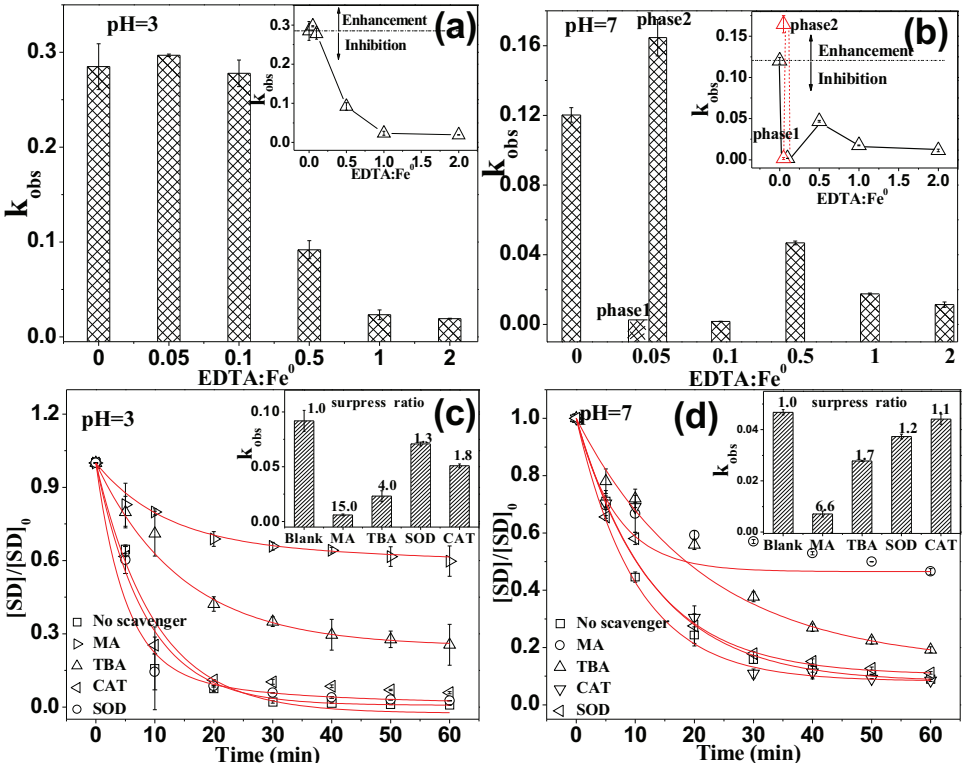

Fig. 5. Effect of (a, b) EDTA dosage and (c, d) 4 scavengers on the SD degradation in the Sono-FL system with pH_0 3.00 or 7.00, respectively. Insets of (a, b): trends of k_{obs}(SD) with EDTA dosage, and insets of (c, d): suppress ratios of SD degradation with four scavengers; (conditions: 0.47 mM EDTA, 20 mg L^{-1} SD, 1.90 mM PS, 0.94 mM Fe^0, 20 W US, 20 °C).

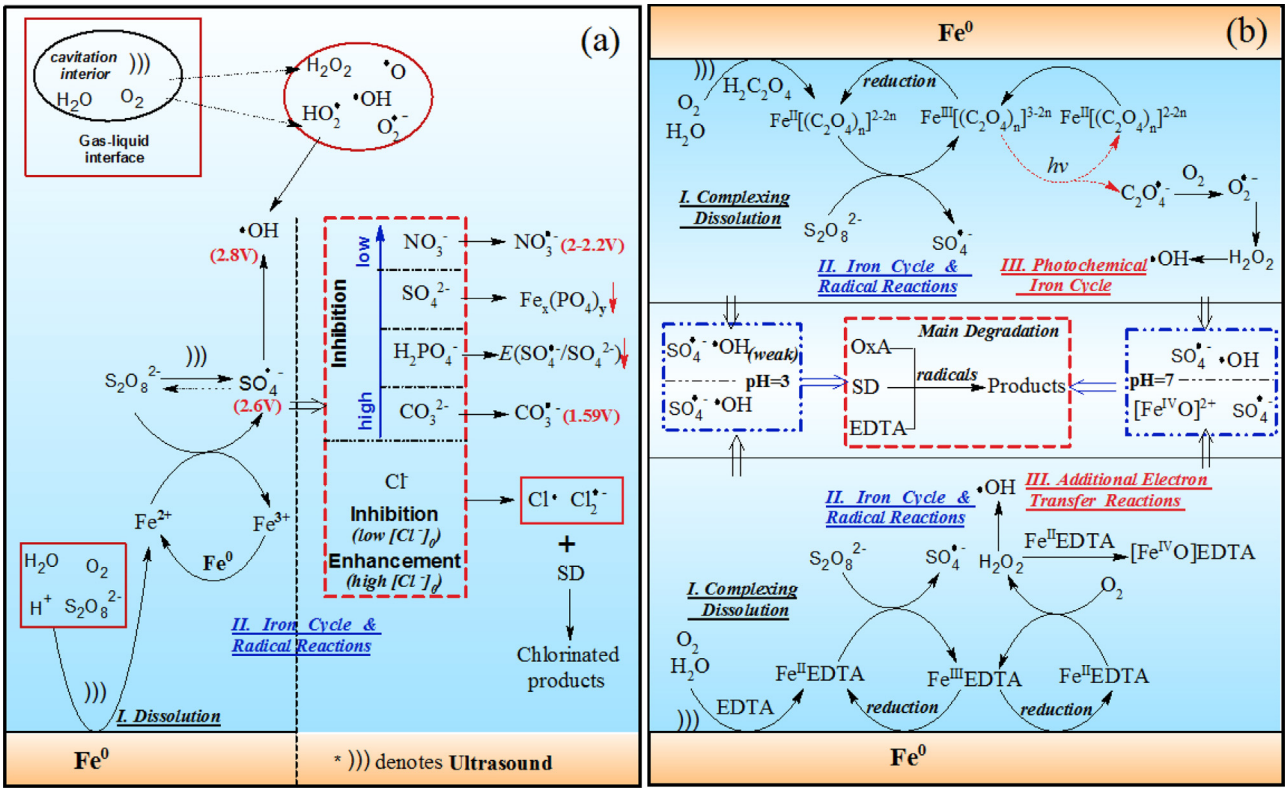

Fig. 6. Proposed mechanistic roles of (a) inorganic anions and (b) chelating agents in interfering the SD degradation in the Sono-FL system.

contribute to the SD degradation in the neutral circumstance. It was expected that the external photochemical reduction of Fe^{III}-OxA ligands would supply additional ROS (i.e., •OH, $O_2^{\bullet-}$ and H_2O_2) [58,60] for the SD degradation. However, it was found that the process might be neglected because the Fe^{II}-OxA complexes would be predominant in the presence of abundant fresh Fe^0 surface area. In addition, OxA could also consume $SO_4^{\bullet-}$ or •OH as others as a competitive pollutant of SD. Concentrated OxA would strongly inhibit the SD degradation due to the related high reaction rates (k(oxalate/$SO_4^{\bullet-}$) = 1.1×10^6 L mol^{-1} s^{-1}, k(oxalate/•OH) = 1.4×10^6 L mol^{-1} s^{-1}) [36,69].

Mechanism in the Sono-FL(EDTA) system would be also mainly composed of three parts: (I) EDTA-complexion dissolution of Fe^0 surface, (II) the iron cycle and sulfate radical reactions, and (III) additional electron transfer reactions between Fe^{II}-EDTA ligand and O_2 for production of ROS. The mechanism part I and part II were similar to that of the Sono-FL(OxA) system. Nevertheless, the mechanism of part III should be different in acidic or neutral circumstance. •OH would be the main generated radical in the former case while [Fe^{IV}O]EDTA would be the main oxidant in the latter case. Concentrated EDTA could also compete with SD for consuming the generated oxidants $SO_4^{\bullet-}$ or •OH [36,67].

4. Conclusion

A novel sonochemical Fe^0-catalyzed Fenton-like system has been investigated for the degradation of antibiotic sulfadiazine. Response surface methodology has been used for optimizing the experimental parameters and an optimal condition of pH 7.00, 0.94 mM Fe^0, 1.90 mM PS and 20 W US power was obtained. Adopting the optimized parameters, the interference and mechanistic roles of the wastewater matrix on the SD degradation were further studied for the Sono-FL system.

It was revealed that most of the studied inorganic anions (SO_4^{2-}, NO_3^-, HCO_3^-/CO_3^{2-}, $H_2PO_4^-$) and chelating agents (EDTA and OxA) would mainly inhibit the SD degradation at different concentration levels. The SD degradation in the system would be enhanced with 5 mM Cl^-, but slightly inhibited with 100 mM Cl^-. Moreover, unexpected chlorinated intermediates/products were also found. Besides, we have found that the Sono-FL system could effectively degrade SD degradation in all cases, even if concentrated wastewater matrix were added. The result suggested that the Sono-FL system could be an appropriate AOP for the treatment of wastewaters with complex characteristics, as compared to •OH-based AOPs. However, its practical applications in treating various industrial wastewaters are still expected to be further investigated.

Acknowledgements

The authors acknowledge the financial support by the National Natural Science Foundation of China (No. 21407052), the Key Project in the National Science & Technology Pillar Program during the Twelfth Five-year Plan Period (2015BAB01B04), Research Fund for the Doctoral Program of Higher Education of China (No. 201225542013), the Fundamental Research Funds for the Central Universities (No. 2014QN144), and SRF for ROCS and SEM.

Appendix A. Supplementary data

Supplementary data associated with this article can be found, in the online version, at http://dx.doi.org/10.1016/j.apcatb.2015.12.004.

References

[1] Y. Segura, F. Martínez, J.A. Melero, Appl. Catal. B 136–137 (2013) 64–69.
[2] N. De la Cruz, R.F. Dantas, J. Giménez, S. Esplugas, Appl. Catal. B 130–131 (2013) 249–256.
[3] Y. Segura, F. Martínez, J.A. Melero, R. Molina, R. Chand, D.H. Bremner, Appl. Catal. B 113–114 (2012) 100–106.
[4] F.J. Beltrán, P. Pocostales, P.M. Álvarez, F. López-Piñeiro, Appl. Catal. B 92 (2009) 262–270.
[5] T. Olmez-Hanci, I. Arslan-Alaton, Chem. Eng. J. 224 (2013) 10–16.
[6] D. Hou, R. Goei, X. Wang, P. Wang, T.T. Lim, Appl. Catal. B 126 (2012) 121–133.
[7] P. Hu, M. Long, Appl. Catal. B 181 (2016) 103–117.
[8] X. Zou, T. Zhou, J. Mao, X. Wu, Chem. Eng. J. 257 (2014) 36–44.
[9] Z. Guo, F. Zhou, Y. Zhao, C. Zhang, F. Liu, C. Bao, M. Lin, Chem. Eng. J. 191 (2012) 256–262.
[10] S. Yang, P. Wang, X. Yang, L. Shan, W. Zhang, X. Shao, R. Niu, J. Hazard. Mater. 179 (2010) 552–558.
[11] A. Ghauch, G. Ayoub, S. Naim, Chem. Eng. J. 228 (2013) 1168–1181.
[12] A. Ghauch, A.M. Tuqan, N. Kibbi, Chem. Eng. J. 197 (2012) 483–492.
[13] A. Ghauch, A.M. Tuqan, N. Kibbi, Chem. Eng. J. 279 (2015) 861–873.
[14] Y. Ren, L. Lin, J. Ma, J. Yang, J. Feng, Z. Fan, Appl. Catal. B 165 (2015) 572–578.
[15] A. Ghauch, A.M. Tuqan, N. Kibbi, S. Geryes, Chem. Eng. J. 213 (2012) 259–271.
[16] Q. Yang, H. Choi, Y. Chen, D.D. Dionysiou, Appl. Catal. B 77 (2008) 300–307.
[17] I. Hussain, Y. Zhang, S. Huang, X. Du, Chem. Eng. J. 203 (2012) 269–276.
[18] H. Li, J. Wan, Y. Ma, Y. Wang, M. Huang, Chem. Eng. J. 237 (2014) 487–496.
[19] S. Rodriguez, L. Vasquez, D. Costa, A. Romero, A. Santos, Chemosphere 101 (2014) 86–92.
[20] S.Y. Oh, H.W. Kim, J.M. Park, H.S. Park, C. Yoon, J. Hazard. Mater. 168 (2009) 346–351.
[21] S.Y. Oh, S.G. Kang, P.C. Chiu, Sci. Total Environ. 408 (2010) 3464–3468.
[22] F.H. Ling, H.M. Hung, M.R. Hoffmann, Environ. Sci. Technol. 34 (2000) 1758–1763.
[23] X. Xiong, B. Sun, J. Zhang, N. Gao, J. Shen, J. Li, X. Guan, Water Res. 62 (2014) 53–62.
[24] Q. Yang, H. Choi, S.R. Al-Abed, D.D. Dionysiou, Appl. Catal. B 88 (2009) 462–469.
[25] R.H. Myers, D.C. Montgomery, C.M. Anderson-Cook, Response Surface Methodology: Process and Product Optimization Using Designed Experiments, John Wiley & Sons, 2009.
[26] Q. Yang, Y. Zhong, H. Zhong, X. Li, W. Du, X. Li, R. Chen, G. Zeng, Process Saf. Environ. Prot. 98 (2015) 268–275.
[27] L. Yue, L. Wang, F. Shi, J. Guo, J. Yang, J. Lian, X. Luo, J. Ind. Eng. Chem. 21 (2015) 971–979.
[28] M.E.T. Sillanpää, Biogeochemistry of chelating agents, Washington, DC, in: B. Nowack, J.M. Briesen (Eds.), American Chemical Society Symposium Series, 910, 2005, pp. 226–233.
[29] E. Lipcynska-Kochany, G. Sprah, S. Harms, Chemosphere 30 (1995) 9–20.
[30] L.G. Devi, K.S.A. Raju, S.G. Kumar, K.E. Rajashekhar, J. Taiwan Inst. Chem. Eng. 42 (2011) 341 –349.
[31] X. Xue, K. Hanna, C. Despas, F. Wu, N. Deng, J. Mol. Catal. A: Chem. 311 (2009) 29–35.
[32] C. Liang, Z.S. Wang, N. Mohanty, Sci. Total Environ. 370 (2006) 271–277.
[33] X. Wu, X. Gu, S. Lu, Z. Qiu, Q. Sui, X. Zang, Z. Miao, M. Xu, Sep. Purif. Technol. 147 (2015) 186–193.
[34] K. Hanna, T. Kone, G. Medjahdi, Catal. Commun. 9 (2008) 955–959.
[35] T. Zhou, T.T. Lim, X. Lu, Y. Li, F.-S. Wong, Sep. Purif. Technol. 68 (2009) 367–374.
[36] T. Zhou, T.T. Lim, X. Wu, Water Res. 45 (2011) 2915–2924.
[37] Y.G. Adewuyi, M.A. Khan, Chem. Eng. J. 281 (2015) 575–587.
[38] I. Sanchez, F. Stuber, J. Font, A. Fortuny, A. Fabregat, C. Bengoa, Chemosphere 68 (2007) 338–344.
[39] B. Li, L. Li, K. Lin, W. Zhang, S. Lu, Q. Luo, S.S. Abu Amr, Ultrason. Sonochem. 20 (2013) 855–863.
[40] F. Guzman-Duque, C. Petrier, C. Pulgarin, G. Penuela, R.A. Torres-Palma, Ultrason. Sonochem. 18 (2011) 440–446.
[41] T. Zhou, X. Wu, Y. Zhang, J. Li, T.T. Lim, Appl. Catal. B 136–137 (2013) 294–301.
[42] S.S. Abu Amr, H.A. Aziz, M.N. Adlan, Waste Manag. 33 (2013) 1434–1441.
[43] I. Mangili, M. Lasagni, K. Huang, A.I. Isayev, Chemom. Intell. Lab. Syst. 144 (2015) 1–10.
[44] P. Neta, R.E. Huie, J. Phys. Chem. 90 (1986) 4644–4648.
[45] C. Liang, Z.S. Wang, C.J. Bruell, Chemosphere 66 (2007) 106–113.
[46] R. Yuan, S.N. Ramjaun, Z. Wang, J. Liu, J. Hazard. Mater. 196 (2011) 173–179.
[47] J. De Laat, T.G. Le, Appl. Catal. B 66 (2006) 137–146.
[48] G.D. Fang, D.D. Dionysiou, Y. Wang, S.R. Al-Abed, D.M. Zhou, J. Hazard. Mater. 227–228 (2012) 394–401.
[49] O. Daniel Maírtire, A. Janina Rosso, Sonia Bertolotti, Galo Carrillo Le Roux, M. Andreí Braun, M.n.C. Gonzalez, J. Phys. Chem. A 105 (2001) 5385–5392.
[50] P. Maruthamuthu, P. Neta, J. Phys. Chem. 82 (1978) 710–713.
[51] P. Maruthamuthu, P. Neta, J. Phys. Chem. 81 (1977) 1622–1625.
[52] C.-H. Weng, H. Tao, Arab. J. Chem. (2015), http://dx.doi.org/10.1016/j.arabjc.2015.05.012.
[53] Y. Liu, J. Wang, J. Hazard. Mater. 250–251 (2013) 99–105.
[54] Y. Wang, J.B. Liang, X.D. Liao, L.-S. Wang, C.L. Teck, J. Dai, Y.W. Ho, Ind. Eng. Chem. Res. 49 (2010) 3527–3532.
[55] M. Marchesi, R. Aravena, K.S. Sra, N.R. Thomson, N. Otero, A. Soler, S. Mancini, Sci. Total Environ. 433 (2012) 318–322.
[56] K. Pirkanniemi, S. Metsarinne, M. Sillanpaa, J. Hazard. Mater. 147 (2007) 556–561.

[57] F.B. Li, Z. Li, C.S. Liu, X.M. Li, T.X. Liu, Ind. Eng. Chem. Res. 46 (2007) 781–787.
[58] F.L. Qing Lan, C. Liu, X.-Z. Li, Environ. Sci. Technol. 42 (2008) 7918–7923.
[59] P. Mazellier, B. Sulzberger, Environ. Sci. Technol. 35 (2001) 3314–3320.
[60] M.E. Balmer, B. Sulzberger, Environ. Sci. Technol. 33 (1999) 2418–2424.
[61] R.E. Huie, C.L. Clifton, Int. J. Chem. Kinet. 28 (1996) 195–199.
[62] P. Neta, R.E. Huie, A.B. Ross, J. Phys. Chem. Ref. Data 17 (1988) 1027.
[63] G.V. Buxton, C.L. Greenstock, W.P. Helman, A.B. Ross, W. Tsang, J. Phys. Chem. Ref. Data 17 (1988) 513.
[64] S.L. Atalla, L.H. Toledo-Pereyra, G.H. MacKenzie, J.P. Cederna, Transplantation 40 (1985) 549–584.
[65] T. Zhou, T.T. Lim, Y. Li, X. Lu, F.S. Wong, Chemosphere 78 (2010) 576–582.
[66] B. Nowack, L. Sigg, J. Colloid Interface Sci. 177 (1996) 106–121.
[67] C. Liang, C.P. Liang, C.C. Chen, J. Contam. Hydrol. 106 (2009) 173–182.
[68] M.C. Ballesteros, E.H. Rueda, M.A. Blesa, J. Colloid Interface Sci. 201 (1998) 13–19.
[69] N. Getoff, F. Schworer, V.M. Markovic, K. Sehested, S.O. Nielsen, J. Phys. Chem. 76 (1971) 749–755.